Topology determination and functional analysis of the *Escherichia coli* TatC protein

Kamila Gouffi, Claire-Lise Santini, Long-Fei Wu*

Laboratoire de Chimie Bactérienne, UPR9043, Institut de Biologie Structurale et Microbiologie, CNRS, 31 chemin Joseph Aiguier, F-13402 Marseille Cedex 20, France

Received 3 April 2002; revised 29 June 2002; accepted 29 June 2002

First published online 17 July 2002

Edited by Gunnar von Heijne

Abstract The TatC protein is an essential component of the bacterial Tat system. By using alkaline phosphatase and β-glucuronidase fusions we found that TatC contains four transmembrane helices. Three insertions of Ala-Ser dipeptide at the cytoplasmic N- and C-termini and in the cytoplasmic loop had no or only partial effect on the TatC function. In contrast, five of seven insertions in the two periplasmic loops abolished the Tat function. Four insertions analyzed had no effect on the stability of the altered TatC proteins or on membrane assembly of the TatA and TatB proteins. These data provide a novel base for more detailed studies of the mechanism of the Tat system.

Key words: TatC; PhoA; UidA; Topology; Folded protein; Tat system

1. Introduction

The bacterial Tat system has a remarkable ability to transport folded proteins even enzyme complexes across the cytoplasmic membrane [1,2]. It is structurally and mechanistically similar to the ΔpH-driven thylakoidal protein import pathway [3–5]. A functional Tat system or ΔpH-dependent pathway requires three integral membrane proteins: TatA/Tha4, TatB/Hcf106 and TatC/cpTatC [6–13]. The TatC protein is essential for the function of both pathways. It might be involved in twin-arginine signal peptide recognition [1,14], protein translocation [2,15] and proton translocation [16]. Sequence analysis predicts that TatC contains six transmembrane helices (TMHs) [8,13,17–19], and experimental data confirmed that N- and C-termini of TatC or cpTatC are exposed to the cytoplasmic or stromal face of the membrane [13,15,19]. Recently, two independent studies using site-directed mutagenesis revealed that the cytoplasmic N-terminus and the first cytoplasmic loop region of the *Escherichia coli* TatC protein are essential for protein export [17,18]. In addition, cross-complementation experiments revealed that at least two TatC molecules co-exist within each Tat translocon [17].

In this study, we assessed the topology of the *E. coli* TatC protein by using the periplasmic alkaline phosphatase (PhoA) and the cytoplasmic β-glucuronidase (UidA) reporter proteins. We found that the second predicted cytoplasmic loop is in fact located in the periplasm, hence TatC likely contains only four TMHs. In addition, by insertion of Ala-Ser dipeptide at the predicted cytoplasmic or periplasmic regions, we found that the TatC function was tolerant to the insertion in the N- and C-terminal regions and in the cytoplasmic loop. In contrast, five of seven insertions in the first and the second periplasmic loops completely abolished the TatC function. Therefore, in addition to the N-terminus and the cytoplasmic loop, our data indicate that the periplasmic loops of the TatC protein are also essential for protein export. Moreover, we observed that the four insertions analyzed affected neither the stability of the altered TatC proteins nor the membrane assembly of the TatA and TatB proteins whatever the TatC function was impaired or not.

2. Materials and methods

2.1. Bacterial strains, plasmids and media

E. coli strains used in this study are: MC4100A (F′ *lacΔU169 araD139 rpsL150 thi flbB5301 deoC7 ptsF25 relA1 ara*$^+$), DADEA (as MC4100A, Δ*tatABCDE*) [20], TG1 (Δ(*lac-pro*) *supE thi hsdD5*/F′ *traD36 proA*$^+$*B*$^+$ *lacI*^{q} *lacZ*ΔM15, laboratory stock), CC118 (*ara*Δ139 Δ(*ara, leu*)7697 Δ*lac*X74 *phoA*Δ20 *galE galK thi rpsE rpoB argE*$_{am}$ *recA1*) and EZ4 (*rpsL* Δ(*add-uid-man*)). The plasmids used are pET22b(+) (Novagen), pMOD⟨MCS⟩ (Epicentre), pPB301 (TnTIN (*uidA*$^+$ *neo*$^+$)) and pMM1 (TnTAP (*phoA*$^+$ *neo*$^+$)) [21].

The bacteria were routinely grown in Luria–Bertani (LB) medium, on LB plates or in the minimal M9 media [22]. Anaerobic growth was achieved normally in stoppered bottles or tubes filled to the top or on plates in GasPak anaerobic jars (BBL Microbiology Systems). As required, ampicillin (Amp) (50 μg/ml), kanamycin (Kan) (50 μg/ml), trimethylamine *N*-oxide (TMAO) (1 mg/ml), glycerol (0.5%), ammonium molybdate (1 μM), potassium selenite (1 μM), sodium dodecyl sulfate (SDS) (0.2%) or IPTG (0.5 mM) were added. Pre-cultures were grown from single colonies and used at 100-fold dilutions for inoculation of experimental cultures.

2.2. Mutagenesis of the tatC gene

We attempted to construct random *phoA* fusions by using the in vivo TnTap and TnTin transposition [21]. The TnTap and TnTin are two Tn5-based mini-transposons respectively carrying the bacterial reporter genes *uidA* or signal sequenceless *phoA*, both lacking a promoter and translation initiation signals. When fused to other proteins, the *uidA* gene product, β-glucuronidase, and the *phoA* gene product, alkaline phosphatase, display corresponding enzymatic activities only if they are located in the cytoplasm or periplasm, respectively [21]. The *neo* gene conferring Kan resistance is also present in TnTap and TnTin mini-transposons. The plasmids pMM1 and pPB301 are pACYC184 derivatives carrying Tn5 transposase-encoding gene and TnTap and TnTin, respectively [21]. To construct TatC-PhoA or TatC-UidA fusions via the in vivo transposition, p8737, a pET22b(+) derivative containing *tatABCD* operon and plasmids pPB301 or pMM1 were transformed into strain TG1. After an over-

*Corresponding author. Fax: (33) 491 71 89 14.
E-mail address: wu@ibsm.cnrs-mrs.fr (L.-F. Wu).

0014-5793/02/$22.00
PII: S0014-5793(02)03069-7

night growth, plasmids were purified and digested by enzymes that cleave only pPB301 or pMM1. The restriction digestion products were transformed into strain EZ4 or CC118. The transformed bacteria were analyzed on LB agar indicator plates containing specific dyes, i.e. 5-bromo-4-chloro-3-indolyl β-D-glucuronide (X-GLUC, 40 μg/ml) for UidA activity or 5-bromo-4-chloro-3-indolyl-phosphate (X-P, 40 μg/ml) for PhoA activity [21]. For unknown reasons, none of the colonies resistant to both Amp and Kan showed alkaline phosphatase or β-glucuronidase activity and plasmids isolated from these colonies exhibited aberrant structures when analyzed by various endonuclease restriction enzymes. To circumvent this problem, we adapted the in vitro random insertion procedure to enhance transposition efficiency by using the EZ::TN™ transposase (Epicentre) and the EZ::TN™ pMOD⟨MCS⟩ Transposon Construction Vector. The EZ::TN™ transposase is a hyperactive, mutated form of Tn5 transposase. pMOD⟨MCS⟩ is a small, high-copy number pUC-based *E. coli* plasmid and contains a 63-bp multiple cloning site (MCS) flanked at each end by the hyperactive 19-bp Mosaic End (ME: 5′-AGATGTGTATAAGAGACAG-3′) specifically recognized by EZ::TN™ transposase. To construct a suitable transposable element, the *phoA-neo* cassette was amplified by polymerase chain reaction (PCR) using primers tap-xba (5′-GCTCTAGATTTGCGGCCGCGTCGACCTGCA-3′) and tap-sac (5′-TCCGAGCTCTTTGAAAACCTGTACTTCCAG-3′) and TnTap as template. The PCR product was digested with *Xba*I–*Sac*I and cloned into pMOD⟨MCS⟩ to give pmodTap. The transposable element carrying the *phoA-neo* cassette flanked by hyperactive MEs was amplified by PCR using pmodTap as templates and pmod-fp (5′-CGGAATTCATTCAGGCTGCGCAACTGT-3′) and pmod-rp (5′-CGGGATCCGTCAGTGAGCGAGGAAGCGGAAG-3′) as primers. The random in vitro transposition of the ME-*phoA-neo*-ME transposable element into p8737 was performed by using the EZ::TN transposase according to the manufacturer's instructions (Epicentre, TEBU). The transposition reaction product was then introduced by electroporation into the CC118 strain. Blue ($PhoA^+$) Amp^R and Kan^R colonies were selected on agar plates containing 40 μg/ml of X-P.

Site-specific introduction of the *Nhe*I site at various positions of the *tatC* gene was constructed by using gene splicing by an overlap extension protocol [23]. Briefly, two DNA fragments were amplified in separate PCRs using the oligonucleotides pairs BglIITatAup (5′-GAAGATCTCGATCCCGCGAAATTAATACGACTCAC-3′) and one of the following oligonuecleotides NheI-1-DW (5′-CAGCTCAATCAGATGGCTAGCCGTGATAAGCGGTTG-3′), NheI-2-DW (5′-GGCCACGTCGGTGGCGATGCTAGCCATCGTTGAACC-3′), NheI-3-DW (5′-CAGCAGCGGCACCACGCTAGCCAGGCGACGTTCATG-3′), NheI-4-DW (5′-GTCGGTGGATACGCTAGCCTGCACCCCTTCCGGCGC-3′), NheI-5-DW (5′-GCGTAAGTCTTCTGGGCTAGCCGAGGTAATCCCCAT-3′), NheI-6-DW (5′-CGTTTGCGAGAAGACGCTAGCATCCGGCGGCGTCAG-3′), NheI-7-DW (5′-TTCAGCGTCGTTTTCGCTAGCCTCTTCCCGATTTCG-3′), NheI-170-DW (5′-CACAATTGCTACCGGCACGCTAGCTTCAAAGGAGAC-3′), NheI-180-DW (5′-GGTAATCCCCATGCTAGCCCAGCACAGCAGCAC-3′), NheI-193-DW (5′-CAGCACATACGGGCTAGCGCGTTTTTTGCGTAAGTC-3′), NheI-194-DW (5′-CAGCACATAGCTAGCCGGGCGTTTTTTGCGTAAGTC-3′), in one reaction; and XhopetDW (5′-CCGCTCGAGTGCGGCCGCAAGCTTGTCGACGGAGCT-3′) and one of the following nucleotides NheI-1-UP (5′-CCGCTTATCACGGCTAGCCATCTGATTGAGCTGCGT-3′), NheI-2-UP (5′-GGTTCAACGATGGCTAGCATCGCCACCGACGTGGCC-3′), NheI-3-UP (5′-GAACGTCGCCTGGCTAGCGTGGTGCCGCTGCTGGTT-3′), NheI-4-UP (5′-CCGGAAGGGGTGCAGGCTAGCGTATCCACCGACATC-3′), NheI-5-UP (5′-GGGATTACCTCGGCTAGCCCAGAAGACTTACGCAAA-3′), NheI-6-UP (5′-ACGCCGCCGGATGCTAGCGTCTTCTCGCAAACGCTG-3′), NheI-7-UP (5′-AATCGGGAAGAGGCTAGCGAAAACGACGCTGAAGCA-3′), NheI-170-UP (5′-GGTGTCTCCTTTGAAGCTAGCGTGCCGGTAGCAATT-3′), NheI-180-UP (5′-GTGCTGCTGTGCTGGGCTAGCATGGGGATTACCTCG-3′), NheI-193-UP (5′-TTACGCAAAAAACGCGCTAGCCCGTATGTGCTGGTT-3′), or NheI-194-UP (5′-TTACGCAAAAAACGCCCGGCTAGCTATGTGCTGGTT-3′ in another reaction. The plasmid p8737 was used as template for all these reactions. The two PCR products devoted to create the same *Nhe*I site were then mixed and used together as template for another PCR by using BglIITatAup (5′-GAAGATCTCGATCCCGCGAAATTAATACGACTCAC-3′) and XhopetDW (5′-CCGCTCGAGTGCGGCCGCAAGCTTGTCGACGGAGCT-3′) as primers to generate a *Nhe*I site after T_{11}, M_{59}, L_{106}, Q_{146}, E_{170}, W_{180}, S_{185}, R_{193}, P_{194}, D_{211} and E_{245} of *tatC*. Concomitantly, Ala-Ser dipeptide was inserted at these positions. The PCR products were digested by *Bgl*II and *Xho*I and cloned into the corresponding sites of pET22b(+). All mutations constructed were confirmed by enzymatic digestions and DNA sequencing. *phoA-neo* or *uidA-neo* were amplified with primers NheI-TAP-UP (5′-CTAGCTAGCACCATCATCGATGAATTCGAG-3′) and NheI-TAP-DW (5′-CTAGCTAGCAACCCTGAAGCTTGCATGCCT-3′) by using pmodTAP and pmodTIN as template, and then cloned into each *Nhe*I site. The resulted plasmids were introduced into *E. coli* CC118 or EZ4 and screening for blue colonies on LB agar plates containing Amp, Kan and X-P (for TatC-Tap) or X-GLUC (for TatC-Tin).

2.3. Enzyme assays

Alkaline phosphatase and β-glucuronidase activities were assayed by the hydrolysis respectively of *p*-nitrophenyl phosphate or *p*-nitrophenyl glucuronide and the absorption of the produced *p*-nitrophenol was measured at 410 nm with a Cary 50 spectrophotometer using a control without extract as the reference blank. One unit of enzyme activity is defined as the release of 1 μmol of nitrophenol/min.

2.4. Cellular fractionation, electrophoresis and immunoblot analysis

Cellular fractions were prepared by lysozyme/EDTA/cold osmoshock and ultracentrifugation as described previously [24]. The protein samples resolved on SDS-denaturing gels by electrophoresis and immobilized onto a PVDF membrane were analyzed by immunoblot using the ECL method according to the manufacturer's instructions (Amersham Bioscience).

3. Results

3.1. Assessing the topology of the TatC protein by random transposition of TnTap

The *tatABCD* operon encodes three integral membrane proteins, TatA, TatB and TatC, and one cytoplasmic soluble protein TatD. TatA and TatB comprise a homologous TMH, an adjacent amphipathic helix, and a variable C-terminal re-

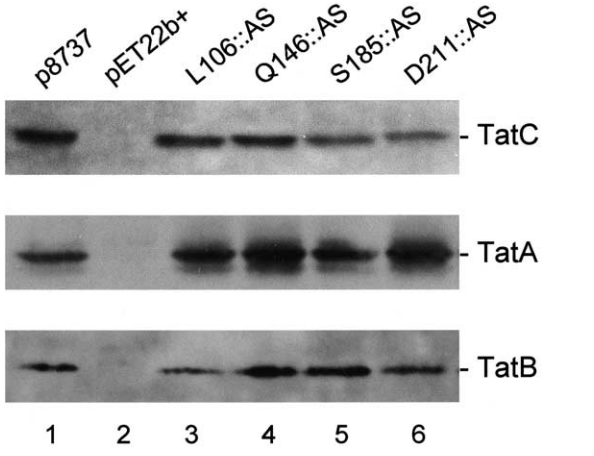

Fig. 1. Stability of the various TatC::AS proteins and membrane assembly of the TatA and TatB proteins. 20 μg of membrane proteins, prepared from the DADEA mutant carrying the vector pET22b(+) (lane 2, negative control), the original plasmid p8737 ((*tatABCD*)$^+$, lane 1) or its derivatives expressing in *trans* the intact TatA and TatB proteins and altered TatC proteins with the Ala-Ser insertions (::AS) at the indicated positions, were separated on 12.5% SDS-denaturing gels and analyzed by immunoblot using antisera at 1/1000-, 1/10 000- and 1/500-fold dilutions against the TatC (upper panel), TatA (middle panel) and TatB (lower panel) proteins, respectively.

gion [7]. TatC is predicted to contain six TMHs [8]. To assess their topology, we constructed PhoA fusions by using the in vitro random transposition protocol (see Section 2). A dozen of colonies showing alkaline phosphatase activity were obtained. Further mapping by endonuclease restriction enzyme digestion, PCR and DNA sequencing analysis revealed that three of them were fused with the TatC protein at positions alanine 125 ($TatC_{A125}$), tyrosine 126 ($TatC_{Y126}$) and leucine 207 ($TatC_{L207}$). The three fusions are located in the third and fifth predicted TMHs both with an in–out orientation.

3.2. Insertion of Ala-Ser dipeptide in the predicted cytoplasmic and periplasmic regions

Since the in vitro random transposition frequency was rather low and the three PhoA fusions obtained were all located in the predicted TMHs, we sought to define the TatC topology by site-specific fusions of PhoA and UidA. The fusion constructions were achieved by a two-step procedure. At first step, we introduced the endonuclease restriction enzyme *Nhe*I cleavage site, with concomitant insertion of an alanine and a serine, after the codons encoding Thr at position 11 ($TatC_{T11::AS}$), Met at 59 ($TatC_{M59::AS}$), Leu at 106 ($TatC_{L106::AS}$), Gln at 146 ($TatC_{Q146::AS}$), Ser at 185 ($TatC_{S185::AS}$), Asp at 211 ($TatC_{D211::AS}$) and Glu at 245 ($TatC_{E245::AS}$) (see Section 2). The reason for this strategy was that these residues were predicted to be located in the extreme N- and C-terminal regions and in the cytoplasmic or periplasmic loops. Some of the insertion sites are in the highly conserved regions of TatC. We could thus firstly assess the impact of these insertions on TatC function and secondly define the topology of TatC by constructing PhoA or UidA fusions at these positions. A standard means for assaying for Tat function is to test for anaerobic growth on TMAO minimal media [6–8,25]. Because they have negligible levels of periplasmic TMAO reductase (TorA) and membrane-bound dimethyl sulfoxide reductase (DmsABC) activities, Δ*tatC* mutants are incapable of anaerobic growth with TMAO as sole electron acceptor unless they are complemented in *trans* by a functional *tatC* gene [8,17,18]. We analyzed the growth of the DADEA (Δ*tatABCDE*) mutant transformed with various plasmids carrying the intact *tatA*, *tatB* and *tatD* genes and the altered *tatC* gene. As shown in Table 1, the strains carrying the plasmids encoding $TatC_{T11::AS}$, $TatC_{S185::AS}$ and $TatC_{E245::AS}$ grew normally as the positive control strain containing the original plasmid p8737. Therefore, these insertions have no effect on the TatC function. The $TatC_{L106::AS}$ insertion slowed down the growth by increasing about six-fold the doubling time, but without effect on maximal yield. In marked contrast, the Ala-Ser insertions at M_{59} ($TatC_{M59::AS}$), Q146 ($TatC_{Q146::AS}$) and D211 ($TatC_{D211::AS}$) completely abolished the TatC function (Table 1).

Another phenotype of the Δ*tatC* mutant is that it cannot grow in media containing SDS [17,26]. The ability of the altered *tatC* genes to restore SDS resistance was assessed (Table 1). All but one Ala-Ser insertions exhibited SDS sensitivity phenotypes that were fully consistent with the capacity of growth on TMAO minimal media. The altered *tatC* genes conferring the Δ*tatC* mutant resistant to SDS restored the

Table 1
Characteristics of Ala-Ser insertion and fusion mutants of the TatC proteins

Plasmids (altered *tatC* genes[a])	Growth on TMAO[b]	SDS sensitivity[b]	PhoA activity[c]	UidA activity[c]
p8737 ((*tatABCD*)$^+$)	+	resistant	17	11
p9937 ($tatC_{T11::AS}$)	+	resistant	ND	ND
p9937Tin ($tatC_{T11}$-*uidA*)	−	sensitive	ND	10 929
p9938 ($tatC_{M59::AS}$)	−	sensitive	ND	ND
p9938Tap ($tatC_{M59}$-*phoA*)	−	sensitive	5 465	ND
p9939 ($tatC_{L106::AS}$)	+/−	sensitive	ND	ND
p9939Tin ($tatC_{L106}$-*uidA*)	NA	NA	ND	13 661
pE21 ($tatC_{A125}$-*phoA*)	−	sensitive	12 902	ND
pF31 ($tatC_{Y126}$-*phoA*)	−	sensitive	12 504	ND
p9940 ($tatC_{Q146::AS}$)	−	sensitive	ND	ND
p9940Tap ($tatC_{Q146}$-*phoA*)	−	sensitive	10 382	ND
p9944 ($tatC_{E170::AS}$)	−	sensitive	ND	ND
p9944Tap ($tatC_{E170}$-*phoA*)	−	sensitive	15 573	ND
p9941 ($tatC_{S185::AS}$)	+	resistant	ND	ND
p9941Tap ($tatC_{S185}$-*phoA*)	−	sensitive	6 557	ND
p9946 ($tatC_{R193::AS}$)	+	resistant	ND	ND
p9946Tap ($tatC_{R193}$-*phoA*)	−	sensitive	2 252	ND
p9947 ($tatC_{P194::AS}$)	−	sensitive	ND	ND
p9947Tap ($tatC_{P194}$-*phoA*)	−	sensitive	7 969	ND
pM6 ($tatC_{L207}$-*phoA*)	−	sensitive	13 104	ND
p9942 ($tatC_{D211::AS}$)	−	sensitive	ND	ND
p9942Tap ($tatC_{D211}$-*phoA*)	−	sensitive	20 765	ND
p9943 ($tatC_{E245::AS}$)	+	resistant	ND	ND
p9943Tin ($tatC_{E245}$-*uidA*)	NA	NA	ND	15 847

[a]The plasmids carrying the *tatC* genes with *Nhe*I site at various positions are indicated by names starting with p99. The further construction of PhoA or UidA fusions from these plasmids at the *Nhe*I sites is indicated by adding Tap or Tin at the end of the corresponding plasmid names, respectively. The PhoA fusions expressed from the plasmids pE21, pF31 and pM6 were constructed by random in vitro transposition.
[b]The DADEA mutants carrying the corresponding plasmids were inoculated in minimal TMAO/glycerol media or in LB media plus 0.2% SDS and incubated at 37°C overnight as described by [17]. Successful growth or not on the minimal TMAO media or LB+SDS is indicated by + or resistant and − or sensitive, respectively. Unlike the negative control, the mutant expressing $TatC_{L106::AS}$ displayed a significant growth, but the doubling time increased by six-fold compared to the positive control. The slowed-down growth is indicated by +/− here. NA means non-applicable since the corresponding strains could not be constructed.
[c]PhoA and UidA activities detected in CC118 or EZ4, respectively, carrying the plasmids as indicated, were performed as described in Section 2. ND: not determined.

growth on the TMAO media and vice versa. However, the $TatC_{L106::AS}$ represented an exception, which could not restore the resistance to SDS but allowed the growth on TMAO minimal media. Interestingly, the $TatC_{L106::AS}$ insertion is close to the essential residue Glu-103, of which the E103Q substitution led to the similar consequence as L106::AS insertion, partial growth on TMAO minimal media, but remains sensitive to SDS [17]. In contrast, the E103A substitution could restore neither the growth on the TMAO minimal media nor resistance to SDS [17]. Remarkably, the D211A mutant exhibits a phenotype completely opposite to those of the E103Q substitution or the $TatC_{L106::AS}$ insertion mutants; it cannot grow on the TMAO minimal media but is resistant to SDS [17]. Since the mechanism of sensitivity to SDS of the *tat* mutants is unknown, at present we have no explanation for the discrepancy regarding these phenotypes.

The growth data showed that Ala-Ser insertions led to different consequences with respect to TorA export. To address the question whether these insertions could disturb the synthesis or have any effect on the stability of the altered TatC, we analyzed the level of the mutant TatC proteins expressed in *trans* together with the intact *tatABD* genes in the DADEA (Δ*tatABCDE*) mutant. The plasmid p8737 ((*tatABCD*)$^+$) or the vector pET22b(+) were used as the positive and the negative controls, respectively. As shown in Fig. 1, membrane fractions of various strains contained similar levels of the TatC protein. Moreover, similar levels of TatA or TatB were detected in these samples (Fig. 1). Therefore, the insertions have significant effect neither on the stability of the TatC protein, nor on the membrane assembly of the TatA and TatB proteins.

3.3. Determination of the TatC topology by the PhoA and UidA fusions

We further assessed the topology of the *E. coli* TatC protein by cloning *phoA-neo* and *uidA-neo* cassettes at the seven *Nhe*I sites located in four predicted cytoplasmic regions and three predicted periplasmic loop regions (see Section 2). Notably, cloning at positions T11, L106 and E245 only resulted in the β-glucuronidase (UidA) activity, whereas cloning at positions M59, Q146 and D211 led to alkaline phosphatase (PhoA) activity exclusively (Table 1). These results confirmed thus that T11, L106 and E245 are located in the cytoplasmic regions and M59, Q146 and D211 are exposed to the periplasm. Strikingly, only PhoA fusion, but not UidA fusion was obtained at position S185 (Table 1), which is predicted to be located in the second cytoplasmic loop. Therefore, in contrast to the prediction, S185 is exposed to the periplasm but not to the cytoplasm. Together with the three PhoA fusions obtained by in vitro transposition, these results revealed that the *E. coli* TatC protein is composed of one cytoplasmic loop and two periplasmic loops that connect four TMHs (Fig. 2).

Among the seven PhoA fusions, the alkaline phosphatase activities of $TatC_{M59-PhoA}$ and $TatC_{S185-PhoA}$ were about half those of others (Table 1). To confirm the fusion construction and to gain explanation for the lower PhoA activity, we analyzed by immunoblot the stability of the seven PhoA fusions obtained in this study. Comparing to the control Δ*tatABCDE*/

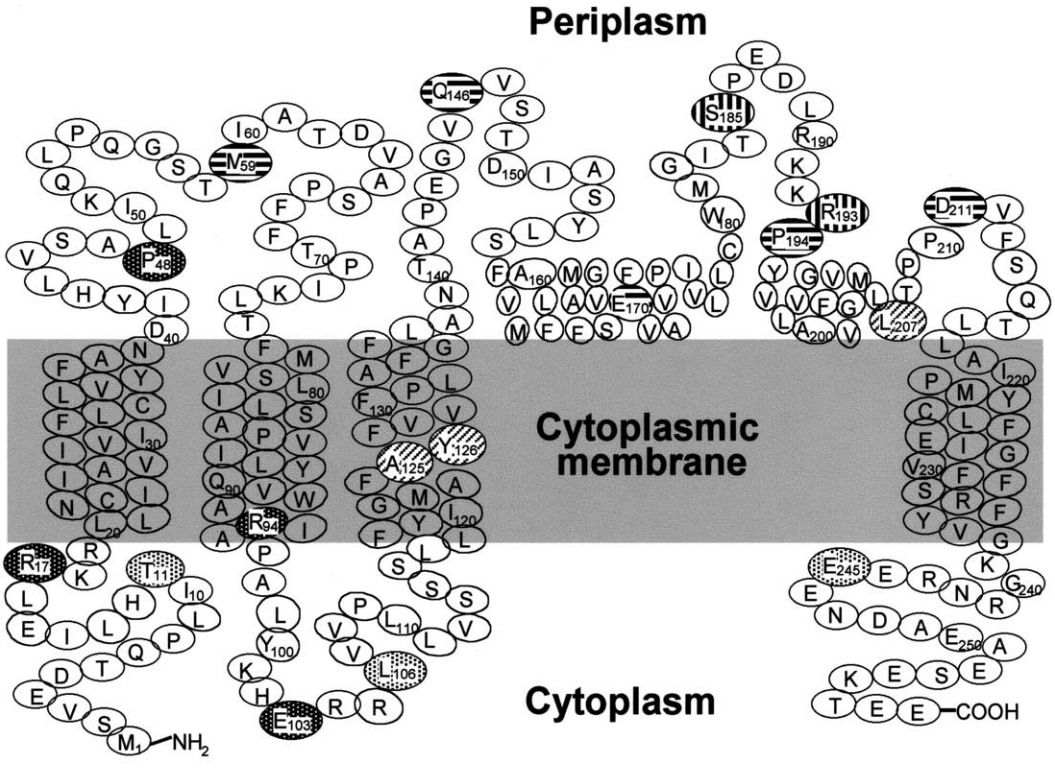

Fig. 2. Topology of the *E. coli* TatC protein determined by using PhoA and UidA fusions. The three UidA fusions ($T_{11-UidA}$, $L_{106-UidA}$ and $E_{245-UidA}$) are indicated by black dots over white background motifs. The 10 PhoA fusions are indicated by linear motifs; horizontal lines indicate that the Ala-Ser insertions at the corresponding positions ($M_{59::AS}$, $Q_{146::AS}$, $R_{170::AS}$, $P_{194::AS}$ and $D_{211::AS}$) blocked the TorA export, the vertical line means that the corresponding Ala-Ser insertion ($E_{193::AS}$ and $S_{185::AS}$) had no effect on TorA export and such data are not available for diagonal lines. The residues with white dots over black background (R_{17}, P_{48}, F_{94} and E_{103}) and D_{211} are those that have been established as essential for the TatC function by [17,18].

p8737, in *trans* expression of the various *tatC-phoA* genes all resulted in the detection of TatC-PhoA fusion proteins with apparently expected sizes (Fig. 3A). However, three fusions, $TatC_{M59-PhoA}$, $TatC_{S185-PhoA}$ and $TatC_{D211-PhoA}$, were unstable (Fig. 3A, lanes 2, 6 and 8). Therefore, the labile nature of $TatC_{M59-PhoA}$ and $TatC_{S185-PhoA}$ could account for the lower PhoA activities of these two fusion proteins (Table 1). Notably, none of these TatC-PhoA fusions could rescue the growth on minimal TMAO media or the sensitivity to SDS of the DADEA mutant (Table 1).

In parallel, we analyzed whether the TatC-UidA fusions could restored the Δ*tatC* phenotype. The $TatC_{T11-UidA}$ could not complement the Δ*tatC* mutation. Moreover, it did not disturb cellular growth in rich medium (data not shown), indicating that the expression of the fusion is not toxic. In marked contrast, we could not transform the DADEA mutant with the plasmids p9939Tin ($TatC_{L106-UidA}$) or p9943Tin ($TatC_{E245-UidA}$), suggesting a lethal effect of in *trans* expression of these two cytoplasmic UidA fusions in the mutant. In contrast, the two plasmids were transformed into the wild-type parental strain without any difficulty. Therefore, unlike Ala-Ser insertions or other fusions, in *trans* expression of $TatC_{L106-UidA}$ and $TatC_{E245-UidA}$ seems to have a toxic effect on the growth of the Δ*tatABCDE* mutant.

3.4. Confirmation of the periplasmic location of the second predicted cytoplasmic loop

The finding of the S185 periplasmic location is surprising since it is on the second predicted cytoplasmic loop between the fourth and fifth TMHs. To confirm this result, an *Nhe*I site was introduced at positions E170 (in the middle of the predicted fourth TMH), W180 (at the end of the predicted fourth TMH), R193 and P194 (in front of the fifth TMH). The resulting Ala-Ser dipeptide insertions $TatC_{E170::AS}$ and $TatC_{P194::AS}$ abolished the TatC function since the DADEA/$pTatC_{E170::AS}$ and DADEA/$pTatC_{P194::AS}$ mutants could not grow on minimal TMAO medium and were sensitive to SDS (Table 1). In contrast, $TatC_{R193::AS}$ restored the wild-type phenotype of the DADEA mutant (Table 1). For unknown reasons, we could not transform the DADEA mutant with the plasmid expressing $TatC_{W180::AS}$ (data not shown). No further experiment was performed with the mutation at the position W180.

The *phoA-neo* cassette was cloned into these *Nhe*I sites and PhoA-positive colonies were obtained. Enzyme essays confirmed that these fusions conferred the host cells significant alkaline phosphatase activity (Table 1). Interestingly, $TatC_{E170}$-PhoA, $TatC_{R193}$-PhoA and $TatC_{P194}$-PhoA exhibited two-fold higher, three-fold lower and similar alkaline phosphatase activities compared to the $TatC_{S185}$-PhoA fusion, respectively. Notably, the two adjacent fusions, $TatC_{R193}$-PhoA and $TatC_{P194}$-PhoA, displayed a three-fold difference in the PhoA activity. The fusion constructions were further confirmed by immunoblot. As shown in Fig. 3B, in *trans* expression of these *tatC-phoA* genes all resulted in the detection of TatC-PhoA fusion proteins (Fig. 3B). However, the fusion proteins showed important differences in their stability. Like the $TatC_{S185}$-PhoA and $TatC_{D211}$-PhoA fusions, the degraded forms of the $TatC_{E170}$-PhoA, $TatC_{R193}$-PhoA and $TatC_{P194}$-PhoA fusion proteins were detected (Fig. 3B, lanes 3, 5 and 6 versus 4 and 7). Moreover, only degraded derivatives were observed for the $TatC_{P194}$-PhoA fusion (Fig. 3B, lane 6). Remarkably, the adjacent $TatC_{R193}$-PhoA fusion was much more stable than $TatC_{P194}$-PhoA. In contrast, the alkaline phosphatase of $TatC_{P194}$-PhoA was three-fold higher than that of $TatC_{R193}$-PhoA (Table 1). The discrepancy between the protein stability and enzymatic activity suggests that the two fusion proteins may be in considerably different conformations or possess different catalytic properties. Collectively, the seven PhoA fusions (at positions Q146, E170, S185, R193, P194, L207 and D211) strongly suggest that the predicted fourth and fifth TMHs and the second cytoplasmic loop are in fact located in the periplasm (Fig. 2).

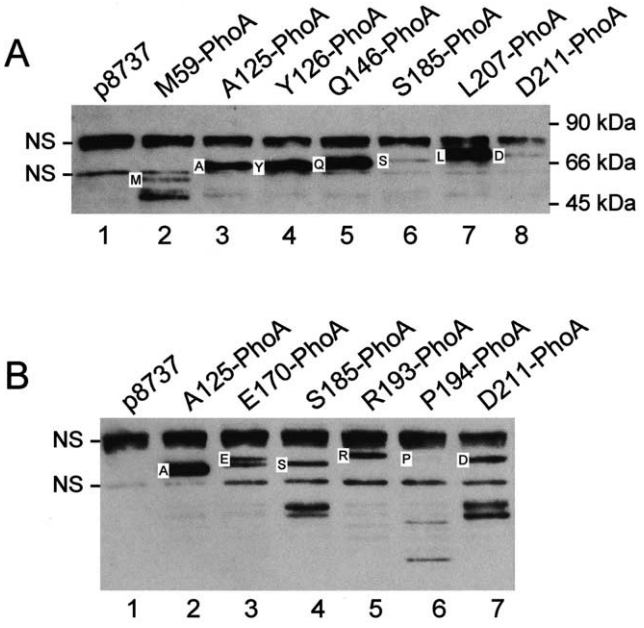

Fig. 3. Stability of various TatC-PhoA fusions. Crude extracts (5 μg protein each) prepared from the DADEA mutant carrying the original plasmid p8737 (lane 1) or its derivatives expressing in *trans* the intact TatA and TatB proteins and altered TatC proteins fused to PhoA at the positions indicated on the top of the panel, were separated on 12.5% SDS-denaturing gels and analyzed by immunoblot using anti-PhoA antisera at 1/10 000-fold dilutions. The TatC-PhoA fusion protein bands are indicated by the one-letter codes of the residues where the PhoA is fused. Molecular weights and the non-specific (NS) bands are indicated on the right and left, respectively. Electrophoresis time and incubation time with anti-PhoA antibodies for the experiment presented in panel B were longer than those presented in panel A.

4. Discussion

E. coli TatC protein is an inner membrane protein composed of 258 amino acids and belongs to the highly conserved TatC family [8]. Four of five methods predict that TatC contains six TMHs with both N- and C-termini located in the cytoplasm, whereas the fifth method suggests that it possesses five membrane spans with a periplasmically exposed C-terminus [19]. Using PhoA and GFP as reporter proteins, Drew et al. have demonstrated a cytoplasmic location of the TatC C-terminus [19]. In this study, we confirmed that the N- and C-termini of TatC are located in the cytoplasm. Remarkably, we found that *E. coli* TatC protein contains one cytoplasmic loop and two periplasmic loops, which could thus connect only four TMHs instead of six as predicted. The best example showing the discrepancy between predicted and experimen-

tally established numbers of TMHs is represented by the topography of the cytochrome *b* of the cytochrome *bc1* complex. Sequence analysis predicts a topology with nine TMHs [27,28], whereas site-specific mutagenesis together with heme binding and functional analysis suggest a topology with eight TMHs [29]. Interestingly, the crystal structure confirms the eight-transmembrane span model and the predicted fourth TMH is extramembranous and run along the membrane surface [30]. Based on these observations, we speculate that the predicted fourth and fifth TMHs of TatC could also be located at the surface, on the periplasmic side of the inner membrane (Fig. 2).

Sequence analysis identified about 30 amino acids that are highly conserved among different TatC proteins. Most of these residues are located in the extreme N-terminal region and in the first predicted cytoplasmic loop [17,18]. The role of these conserved side chains has been assessed by site-directed mutagenesis. The R17A, P48A, F94A, E103A and D211A mutants are completely devoid of Tat-dependent protein export activity and thus represent residues essential for TatC function [17,18]. Given that most essential and important residues cluster around the N-terminus and the first cytoplasmic loop region, the cytoplasmic domains are likely to be essential for the TatC function. In this study, we took another approach to assess the importance of various cytoplasmic and periplasmic regions for the Tat function by inserting Ala-Ser dipeptide at these positions. We reasoned that unlike the site-specific substitutions, the insertion mutation should not have a direct effect on the conserved side chains; rather, it may influence flexibility, hydrophobicity and local conformation of the insertion regions. Interestingly, the insertion in the N-terminus had no effect on the TatC function and the insertion in the cytoplasmic loop near the essential E103 only partially reduced TorA export. Therefore, it implies that the conserved side chains of the residues in these regions are essential for the TatC function. This hypothesis is consistent with the observation that various substitutions for F94 or E103 affect the TatC function differently [17]. The result obtained with $TatC_{E245::AS}$ is fully consistent with the previously observations that the truncation of the *E. coli* TatC protein at R243 or extension of the TatC C-terminus by the addition of a 6His-tag or streptavidin affinity tag have no discernible effect on Tat protein transport [15,17]. Remarkably, the insertions in the middle of the first, and at various positions of the second periplasmically exposed loop regions led to complete loss of Tat-dependent export. The analysis of four insertions revealed that they have no effect on the TatC stability and do not seem to affect the stability and membrane assembly of the TatA and TatB proteins.

The cross-complementation experiments showed that the co-expression of D211A with either F94A or E103A regenerates an active Tat apparatus, and hence leads to the hypothesis that these residues are implicated at different stages of the export process [17]. Furthermore, these results imply that the TatC protein is composed of two functional domains, which are separated by the second periplasmic loop. This loop region seems to be tolerant to various substitutions [17,18]. It has been suggested that D211 plays a structural role in the Tat translocon [17]. Interestingly, whereas the Ala-Ser insertions at positions Q146, R193, P194 and D211 of this loop region completely blocked TorA export, the insertions at positions E170 and S185 had no effect. Importantly, the four Ala-Ser insertions analyzed did not affect the TatC stability or the membrane assembly of the TatA and TatB proteins whether the TatC function was affected or not. Pure speculations for the role of this loop might be its involvement in gating of the Tat channel and/or pushing or pulling the Tat substrates outward across the channel.

Acknowledgements: We thank F. Blasco for valuable discussion regarding the cytochrome *b* topology, M. Ehrmann for the plasmids pMM1 and pBP301, M. Müller and C. Robinson for the antisera against TatC, TatA and TatB. L.-F.W. was supported by 'Quality of Life and Management of Living Resources' Grant QLK3-CT-1999-00917.

References

[1] Berks, B.C., Sargent, F. and Palmer, T. (2000) Mol. Microbiol. 35, 260–274.
[2] Wu, L.-F., Ize, B., Chanal, A., Quentin, Y. and Fichant, G. (2000) J. Mol. Microbiol. Biotechnol. 2, 179–189.
[3] Dalbey, R.E. and Robinson, C. (1999) Trends Biochem. Sci. 24, 17–22.
[4] Settles, A.M. and Martienssen, R. (1998) Trends Cell Biol. 8, 494–501.
[5] Keegstra, K. and Cline, K. (1999) Plant Cell 11, 557–570.
[6] Sargent, F., Bogsch, E.G., Stanley, N.R., Wexler, M., Robinson, C., Berks, B.C. and Palmer, T. (1998) EMBO J. 17, 3640–3650.
[7] Chanal, A., Santini, C.-L. and Wu, L.-F. (1998) Mol. Microbiol. 30, 674–676.
[8] Bogsch, E., Sargent, F., Stanley, N.R., Berks, B.C., Robinson, C. and Palmer, T. (1998) J. Biol. Chem. 273, 18003–18006.
[9] Yahr, T.L. and Wickner, W.T. (2001) EMBO J. 20, 2472–2479.
[10] Settles, A.M., Yonetani, A., Baron, A., Bush, D.R., Cline, K. and Martienssen, R. (1997) Science 278, 1467–1470.
[11] Mori, H., Summer, E.J., Ma, X. and Cline, K. (1999) J. Cell Biol. 146, 45–56.
[12] Walker, M.B., Roy, L.M., Coleman, E., Voelker, R. and Barkan, A. (1999) J. Cell Biol. 147, 267–276.
[13] Mori, H., Summer, E.J. and Cline, K. (2001) FEBS Lett. 501, 65–68.
[14] Cline, K. and Mori, H. (2001) J. Cell Biol. 154, 719–729.
[15] Bolhuis, A., Mathers, J.E., Thomas, J.D., Barrett, C.M. and Robinson, C. (2001) J. Biol. Chem. 276, 20213–20219.
[16] Musser, S.M. and Theg, S.M. (2000) Biochemistry 39, 8228–8233.
[17] Buchanan, G., de Leeuw, E., Stanley, N.R., Wexler, M., Berks, B.C., Sargent, F. and Palmer, T. (2002) Mol. Microbiol. 43, in press.
[18] Allen, S.C., Barrett, C.M., Ray, N. and Robinson, C. (2002) J. Biol. Chem. 277, 10362–10366.
[19] Drew, D.E., Sjostrand, D., Nilsson, J., Urbig, T., Chin, C.-C., de Gier, J.W. and von Heijne, G. (2002) Proc. Natl. Acad. Sci. USA 99, 2690–2695.
[20] Ize, B., Gérard, F., Zhang, M., Chanal, A., Voulhoux, R., Palmer, T., Filloux, A. and Wu, L.-F. (2002) J. Mol. Biol. 317, 327–335.
[21] Ehrmann, M., Bolek, P., Mondigler, M., Boyd, D. and Lange, R. (1997) Proc. Natl. Acad. Sci. USA 94, 13111–13115.
[22] Miller, J.H. (1972) Cold Spring Harbor Laboratory, Cold Spring Harbor, NY.
[23] Horton, R.M., Hunt, H.D., Ho, S.N., Pullen, J.K. and Pease, L.R. (1989) Gene 77, 61–68.
[24] Santini, C.L., Ize, B., Chanal, A., Müller, M., Giordano, G. and Wu, L.-F. (1998) EMBO J. 17, 101–112.
[25] Weiner, J.H., Bilous, P.T., Shaw, G.M., Lubitz, S.P., Frost, L., Thomas, G.H., Cole, J. and Turner, R.J. (1998) Cell 93, 93–101.
[26] Stanley, N.R., Findlay, K., Berks, B.C. and Palmer, T. (2001) J. Bacteriol. 183, 139–144.
[27] Widger, W.R., Cramer, W.A., Herrmann, R.G. and Trebst, A. (1984) Proc. Natl. Acad. Sci. USA 81, 674–678.
[28] Saraste, M. (1984) FEBS Lett. 166, 367–372.
[29] Howell, N. and Gilbert, K. (1988) J. Mol. Biol. 203, 607–618.
[30] Xia, D., Yu, C.A., Kim, H., Xia, J.Z., Kachurin, A.M., Zhang, L., Yu, L. and Deisenhofer, J. (1997) Science 277, 60–66.